Thermodynamics of charged dilatonic BTZ black holes in rainbow gravity

M. Dehghani

Department of Physics, Ilam University, Ilam, Iran

ABSTRACT

In this paper, the charged three-dimensional Einstein's theory coupled to a dilatonic field has been considered in the rainbow gravity. The dilatonic potential has been written as the linear combination of two Liouville-type potentials. Four new classes of charged dilatonic rainbow black hole solutions, as the exact solution to the coupled field equations of the energy dependent space time, have been obtained. Two of them are correspond to the Coulomb's electric field and the others are consequences of a modified Coulomb's law. Total charge and mass as well as the entropy, temperature and electric potential of the new charged black holes have been calculated in the presence of rainbow functions. Although the thermodynamic quantities are affected by the rainbow functions, it has been found that the first law of black hole thermodynamics is still valid for all of the new black hole solutions. At the final stage, making use of the canonical ensemble method and regarding the black hole heat capacity, the thermal stability or phase transition of the new rainbow black hole solutions have been analyzed.

1. Introduction

One of the most outstanding achievements in the various theories of quantum gravity theory, such as string theory [1], loop quantum gravity [2], noncommutative geometry [3] and Gedanken experiments [4], is the prediction of a minimal measurable length in the order of the Planck length [5]. The existence of such a minimal length, which restricts the maximum energy that a particle can attain to the Planck energy, is related to the modification of linear momentum and also quantum commutation relations. Therefore, it can be captured by modification of the usual uncertainty principle known as the generalized uncertainty principle or by promoting the standard energy–momentum relation (i.e. $E^2 - p^2 = m^2$) to the modified dispersion relation. In addition, it is well known that Einstein's general relativity, as an effective theory of gravity, is valid in the infrared limit while it fails to produce accurate results in ultraviolet regime. The gravity's rainbow just like the Horava–Lifshitz gravity theory is motivated by modification of standard dispersion relation in the ultraviolet limit [6]. Such a modification of the geometry at high energy scale can be regarded as the ultraviolet completion of the general relativity. Therefore, gravity's rainbow can be regarded as an attempt to construct the theory of quantum gravity [7].

On the other hand, the modified dispersion relation violates Lorentz invariants. Doubly/Deformed special relativity, as a theory which predicts naturally the modified dispersion relation, is an extension of the special theory of relativity. It has been established based on the nonlinear Lorentz transformations in momentum space. In this theory, the Planck-scale energy beside the speed of light remains invariant. Also the Planck-scale corrected dispersion relation preserves a deformed Lorentz symmetry [8,9]. It is believed that the violation of Lorentz invariancy plays an essential rule in constructing the quantum theory of gravity. Such a Lorentz symmetry violation can occur in the string theory because of the existence of an unstable perturbative string vacuum [10].

Now, the doubly special relativity has been generalized to curved space times and a doubly general relativity or gravity's rainbow has been arrived [11]. In this theory, the geometry of space time depends on the energy of the test particle. Thus, it seems different for the particles having different amounts of energy and the energy dependent metrics form a rainbow of metrics. This is why the double general relativity is named as gravity's rainbow. The modified dispersion relation can be written in the following general form

$$E^2 f^2(\varepsilon) - p^2 g^2(\varepsilon) = m^2, \tag{1.1}$$

where, $\varepsilon = E/E_P$, E_P is the Planck-scale energy, E is the energy of the test particle and the functions $f(\varepsilon)$ and $g(\varepsilon)$ are known as

E-mail address: m.dehghani@ilam.ac.ir.

the rainbow functions, which are required to fulfill the following conditions

$$\lim_{\varepsilon \to 0} f(\varepsilon) = 1, \quad \text{and} \quad \lim_{\varepsilon \to 0} g(\varepsilon) = 1. \tag{1.2}$$

By these requirements one is able to reproduce the standard dispersion relation in the infrared limit. It must be noted that the functional form the rainbow functions are not unique and there are a number of expressions for them which are correspond to different phenomenological motivations. Some of the proposed models for the temporal and spatial rainbow functions can be found in Refs. [12–15].

Nowadays, gravity's rainbow, in which the quantum gravitational effects are taken into account, has attracted a lot of interest and many papers have been appeared in which the physical properties of the black holes are investigated in the presence of rainbow functions. Thermodynamics and phase transition of the modified Schwarzschild black holes via gravity's rainbow are studied in refs. [12,16]. Thermal stability of nonlinearly charged BTZ and four-dimensional rainbow black holes has been analyzed in refs. [7,17]. The effects of rainbow functions on the rotating BTZ black holes are the subject of ref. [18]. Thermodynamics of Gauss–Bonnet black holes in rainbow gravity has been discussed in refs. [19,20]. Also, thermodynamics and stability of the black holes have been studied in the context of massive gravity's rainbow by Hendi et al. [21]. Study of the physics in the energy dependent space times has provided many interesting results such as: back hole remnant [22, 23], Nonsingular universe [24], etc. It is worth noting that there are several other approaches to study the quantum gravity effects on the thermodynamical properties of the black holes. Among them one can see the works of Pourhassan et al. [25–29] and also refs. [30,31].

Recently, study of the impacts of rainbow functions on the black hole thermodynamics and phase transitions have been extended to the case of three-dimensional dilatonic black holes [32], and four-dimensional charged dilatonic black holes [33]. In the same line, and motivated by the fact that modified dispersion relation is one of the quantum gravitational effects, we tend to investigate the thermodynamical properties of some new charged BTZ black holes in the presence of rainbow functions. Regarding to the AdS/CFT correspondence, it is interesting to encode the quantum gravity effects into the black hole solutions in the framework of the rainbow gravity theory. The main goal of the present work is to obtain the modified dilatonic charged BTZ black holes in the energy dependent space times, and to investigate the impacts of rainbow functions on the thermodynamical properties as well as the stability or phase transition of the charged dilatonic BTZ black holes.

The paper is structured as follows: In Sec. 2, by introducing a static spherically symmetric and energy dependent space time, the explicit form of the coupled scalar, electromagnetic and gravitational field equations have been obtained. It has been shown that regarding the relation between the parameters of the theory, two kinds of electric fields are distinguishable, naturally. One is the Coulomb's electric field and the other corresponds to a modified Coulomb law which reduces to the Coulomb's electric field as an especial case. Sec. 3 is devoted to study of the thermodynamical properties of the charged rainbow black hole solutions in the presence of the Coulomb's electric field. Two new classes of charged dilatonic black holes, as the exact solutions to the Einstein–Maxwell-dilaton field equations, have been obtained in the rainbow gravity theory. The conserved and thermodynamical quantities, which are affected by rainbow functions, have been calculated and the validity of the first law of black hole thermodynamics has been proved. Also, making use of the canonical ensemble method, the thermal stability or phase transition of both

of the new black hole solutions has been studied. In Sec. 4, the black hole solutions of the Einstein-dilaton gravity coupled to the modified Coulomb's field have been investigated in the rainbow gravity theory. It has been shown that these field equations also admit two other new black hole solutions. The impacts of rainbow functions on the electric charge and mass as well as the temperature, entropy and electric potential of these new black holes have been calculated too. The validity of the thermodynamical first law and thermal stability of both of the new rainbow black holes have been analyzed. The results are summarized and discussed in Sec. 4.

2. The field equations

The action for three dimensional dilatonic black holes in the presence of Maxwell's electrodynamics can be written in the following general form [32,34–36]

$$I = -\frac{1}{16\pi} \int \sqrt{-g} d^3 x \left[\mathcal{R} - V(\phi) - 2(\nabla \phi)^2 - \mathcal{F} e^{-2\alpha \phi} \right]. \tag{2.1}$$

Here, $\mathcal{R}$ is the Ricci scalar. ϕ is a scalar field and $V(\phi)$ is a self interacting function. The parameter α is the scalar-electromagnetic coupling constant and $\mathcal{F} = F^{\mu\nu} F_{\mu\nu}$ being the Maxwell invariant, $F_{\mu\nu} = \partial_\mu A_\nu - \partial_\nu A_\mu$ and A_μ is the electromagnetic potential. By varying the action (2.1) with respect to the gravitational, electromagnetic and scalar fields, we get the related field equations as follows

$$\mathcal{R}_{\mu\nu} = V(\phi) g_{\mu\nu} + 2\nabla_\mu \phi \nabla_\nu \phi - \left(\mathcal{F} g_{\mu\nu} - 2F_{\mu\alpha} F_\nu^{\ \alpha} \right) e^{-2\alpha \phi}, \tag{2.2}$$

$$\nabla_\mu \left[e^{-2\alpha \phi} F^{\mu\nu} \right] = 0, \tag{2.3}$$

$$4\Box \phi = \frac{dV(\phi)}{d\phi} - 2\alpha \mathcal{F} e^{-2\alpha \phi}, \qquad \phi = \phi(r). \tag{2.4}$$

We consider the following three dimensional energy dependent spherically symmetric geometry [32,33] as the solution to the gravitational field equations (2.2)

$$ds^2 = -\frac{U(r)}{f^2(\varepsilon)} dt^2 + \frac{1}{g^2(\varepsilon)} \left[\frac{dr^2}{U(r)} + r^2 R^2(r) d\theta^2 \right]. \tag{2.5}$$

Assuming as a function of r, the only non-vanishing component of the electromagnetic field is $F_{tr} = -E(r) = h'(r)$, and we have

$$\mathcal{F} = -2f^2(\varepsilon) g^2(\varepsilon) E^2(r) = -2f^2(\varepsilon) g^2(\varepsilon) (h'(r))^2. \tag{2.6}$$

In overall the paper, prime means derivative with respect to the argument.

By combining Eqs. (2.2) and (2.5), we arrived at the following independent differential equations

$$e_{00} \equiv U''(r) + \left(\frac{1}{r} + \frac{R'(r)}{R(r)} \right) U'(r) + \frac{2V(\phi)}{g^2(\varepsilon)} = 0, \tag{2.7}$$

$$e_{11} \equiv e_{00} + 2U(r) \left(\frac{R''(r)}{R(r)} + \frac{2R'(r)}{rR(r)} + 2\phi'^2(r) \right) = 0, \tag{2.8}$$

$$e_{22} \equiv \left(\frac{1}{r} + \frac{R'(r)}{R(r)} \right) U'(r) + \left(\frac{R''(r)}{R(r)} + \frac{2R'(r)}{rR(r)} \right) U(r) + \frac{V(\phi)}{g^2(\varepsilon)} $$
$$+ 2f^2(\varepsilon) F_{tr}^2 e^{-2\alpha \phi} = 0. \tag{2.9}$$

Noting Eqs. (2.7) and (2.8) we obtain

$$\frac{R''(r)}{R(r)} + \frac{2}{r} \frac{R'(r)}{R(r)} + 2\phi'^2(r) = 0. \tag{2.10}$$

The differential equation (2.10) can be written in the following form

$$\frac{2}{r}\frac{d}{dr}\ln R(r) + \frac{d^2}{dr^2}\ln R(r) + \left(\frac{d}{dr}\ln R(r)\right)^2 + 2\phi'^2(r) = 0. \quad (2.11)$$

From Eq. (2.11), one can argue that $R(r)$ must be an exponential function of $\phi(r)$. Therefore, we can write $R(r) = e^{2\beta\phi}$, in Eq. (2.10), and show that $\phi = \phi(r)$ satisfies the following differential equation

$$\beta\phi''(r) + (1 + 2\beta^2)\phi'^2(r) + \frac{2\beta}{r}\phi'(r) = 0. \quad (2.12)$$

It is easy to write the solution of (2.12) in terms of a positive constant b as

$$\phi(r) = \gamma\ln\left(\frac{b}{r}\right), \quad \text{with} \quad \gamma = \frac{\beta}{1 + 2\beta^2}. \quad (2.13)$$

Such a solution has been used previously by Hendi et al. [32,34] and Dehghani [35,36].

3. Black hole solutions with $\beta = \alpha$

Making use of these solutions together with Eqs. (2.3) and (2.5), we have

$$\begin{cases} h(r) = -q\ln\left(\frac{r}{\ell}\right), \\ F_{tr} = -\frac{q}{r}, \end{cases} \quad (3.1)$$

where, q is an integration constant related to the total electric charge on black hole.

Now, Eq. (2.9) can be rewritten as

$$U'(r) - \frac{2\alpha\gamma}{r}U(r) + \frac{r}{1 - 2\alpha\gamma}\left[\frac{V(\phi)}{g^2(\varepsilon)} + 2f^2(\varepsilon)F_{tr}^2 e^{-2\alpha\phi}\right] = 0. \quad (3.2)$$

For solving this equation for the metric function $U(r)$, we need to calculate the scalar functional $V(\phi(r))$ as a function of radial coordinate. To do so, we proceed to solve the scalar field equation (2.4). It can be written as

$$\frac{dV(\phi)}{d\phi} - 4\alpha V(\phi) - 4\alpha f^2(\varepsilon)g^2(\varepsilon)F_{tr}^2 e^{-2\alpha\phi} = 0. \quad (3.3)$$

Now, the first order differential (3.3) can be solved as

$$V(\phi) = \begin{cases} \left(C_1 \pm \frac{4q^2 f^2(\varepsilon)g^2(\varepsilon)}{b^2}\phi\right)e^{\pm 4\phi}, & \text{for} \quad \alpha = \pm 1, \\ \left[C_1 + \frac{2\alpha^2 q^2 f^2(\varepsilon)g^2(\varepsilon)}{b^2(1 - \alpha^2)}e^{\frac{2}{\alpha}(1-\alpha^2)\phi}\right]e^{4\alpha\phi}, \\ \quad \text{for} \quad \alpha \neq \pm 1, \end{cases} \quad (3.4)$$

where C_1 is an integration constant related to the cosmological constant Λ. Noting the fact that in the absence of the dilaton field (i.e. $\phi = 0$), the action (2.1) reduces to the action of Einstein-Λ-Maxwell gravity, the integration constant C_1 can be determined by imposing the condition $V(\phi = 0) = 2\Lambda$.

It leads to $C_1 = 2\Lambda$ and the solutions (3.4) can be written as the following generalized Liouville potentials

$$V(\phi) = \begin{cases} \left(2\Lambda \pm \frac{4q^2 f^2(\varepsilon)g^2(\varepsilon)}{b^2}\phi\right)e^{\pm 4\phi}, & \text{for} \quad \alpha = \pm 1, \\ 2\Lambda_0 e^{4\alpha_0\phi} + 2\Lambda e^{4\alpha\phi}, & \text{for} \quad \alpha \neq \pm 1, \end{cases} \quad (3.5)$$

with

$$\alpha_0 = \frac{1 + \alpha^2}{2\alpha}, \quad \text{and} \quad \Lambda_0 = \frac{\alpha^2 q^2 f^2(\varepsilon)g^2(\varepsilon)}{b^2(1 - \alpha^2)}. \quad (3.6)$$

Now, making use of Eqs. (3.1), (3.2) and (3.5), we obtain the metric function $U(r)$ as

$$U(r) = \begin{cases} -mr^{2/3} - \frac{6}{g^2(\varepsilon)}\left(\frac{r}{b}\right)^{2/3}\left[\Lambda b^2 + q^2 f^2(\varepsilon)g^2(\varepsilon) \right. \\ \left. \times \left(1 + \frac{1}{3}\ln\frac{b^2}{r\ell}\right)\right]\ln\left(\frac{r}{\ell}\right), & \text{for} \quad \alpha = \pm 1, \\ -mr^{2\alpha\gamma} + \frac{(1+2\alpha^2)^2}{g^2(\varepsilon)(\alpha^2-1)}\left[\Lambda r^2\left(\frac{b}{r}\right)^{4\alpha\gamma} \right. \\ \left. + \frac{2q^2 f^2(\varepsilon)g^2(\varepsilon)}{1+2\alpha^2}\left(\frac{b}{r}\right)^{-2\alpha\gamma}\ln\left(\frac{r}{\ell}\right)\right], & \text{for} \quad \alpha \neq \pm 1. \end{cases} \quad (3.7)$$

In the absence of the coupling constant α (i.e. $\alpha = 0$), by taking the infrared limit of the theory, we have

$$U(r) = -m - \Lambda r^2 - 2q^2\ln(r/\ell), \quad (3.8)$$

which is nothing but the metric function of the charged BTZ black holes. Note that m is an integration constant related to the black hole mass. All the field equations are satisfied by the solutions given in this section. The plots of metric functions (3.7) for different values of $f(\varepsilon)$ and $g(\varepsilon)$ have been shown in Figs. 1 and 2.

It is clear that the new rainbow black hole solutions, we obtained here, can show two horizon, extreme and naked singularity black holes. In order to investigate the space time curvature singularities, we need to study the behavior of Ricci and Kretschmann scalars. It is a matter of calculation to show that

$$\lim_{r\to\infty}\mathcal{R} = 0, \quad \text{and} \quad \lim_{r\to 0^+}\mathcal{R} = \infty, \quad (3.9)$$

$$\lim_{r\to\infty}\mathcal{R}^{\mu\nu\rho\lambda}\mathcal{R}_{\mu\nu\rho\lambda} = 0, \quad \text{and} \quad \lim_{r\to 0^+}\mathcal{R}^{\mu\nu\rho\lambda}\mathcal{R}_{\mu\nu\rho\lambda} = \infty. \quad (3.10)$$

Therefore, Ricci and Kretschmann scalars are finite for finite values of the redial component r. There is an essential (not coordinate) singularity located at $r = 0$. Also, the asymptotic behavior of the solutions are neither flat nor A(dS).

In the following section we explore the thermodynamics of the new charged BTZ black hole solutions presented in Eq. (3.7).

3.1. First law of black hole thermodynamics

In this subsection, we would like to check the validity of the first law of black hole thermodynamics for the new three-dimensional rainbow black holes introduced here. The conserved charge of the black hole can be obtained by calculating the total electric flux measured by an observer located at infinity with respect to the horizon (i.e. $r \to \infty$) [37,38], that is

$$Q = \frac{1}{4\pi}\int\sqrt{-g}e^{-2\alpha\phi}F^{tr}d\Omega. \quad (3.11)$$

Making use of Eqs. (3.1) and (3.11) after some simple calculations we arrived at

$$Q = \frac{qf(\varepsilon)}{2}. \quad (3.12)$$

The other conserved quantity to be calculated is the black hole mass. As mentioned before, it can be obtained in terms of the mass parameter m. The Abbott–Deser total mass of the new black holes introduced here can be obtained as [34,39–41]

$$M = \begin{cases} \frac{b^{2/3}}{24 f(\varepsilon)}m, & \text{for} \quad \alpha = \pm 1, \\ \frac{1-2\alpha\gamma}{8 f(\varepsilon)}b^{2\alpha\gamma}m, & \text{for} \quad \alpha \neq \pm 1, \end{cases} \quad (3.13)$$
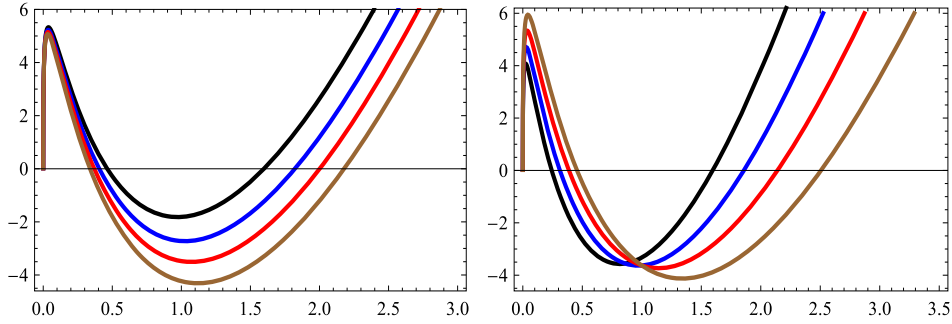
Fig. 1. $U(r)$ versus r for $\alpha = \pm 1$, $\Lambda = -1$, $Q = 1$, $M = 0.2$ and $b = 2$, Eq. (3.7). Left: $g(\varepsilon) = 0.8$ and $f(\varepsilon) = 0.6$, 0.9, 1.15, 1.4 for Black, blue, red, and brown curves, respectively. Right: $f(\varepsilon) = 1.2$ and $g(\varepsilon) = 0.75$, 0.78, 0.81, 0.84 for Black, blue, red, and brown curves, respectively. (For interpretation of the references to color in this figure legend, the reader is referred to the web version of this article.)
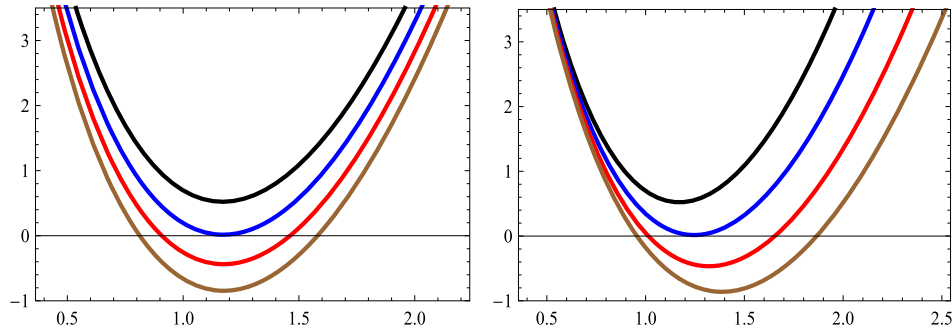

Fig. 2. $U(r)$ versus r for $\alpha \neq \pm 1$, $\Lambda = -1$, $Q = 1$, $M = 0.25$, $\alpha = 0.15$ and $b = 2$, Eq. (3.7). Left: $g(\varepsilon) = 0.6$ and $f(\varepsilon) = 1.25$, 1.525, 1.75, 1.95 for Black, blue, red, and brown curves, respectively. Right: $f(\varepsilon) = 1.28$ and $g(\varepsilon) = 0.6$, 0.635, 0.67, 0.7 for Black, blue, red, and brown curves, respectively. (For interpretation of the references to color in this figure legend, the reader is referred to the web version of this article.)

which is compatible with the mass of charged BTZ black hole when $\varepsilon \to 0$ and the dilatonic potential disappears.

One can obtain the Hawking temperature associated with the black hole horizon in terms of the surface gravity κ. That is

$$
T = \frac{\kappa}{2\pi} = \frac{g(\varepsilon)}{f(\varepsilon)} \frac{U'(r_+)}{4\pi}
$$
$$
= \begin{cases} \frac{3(r_+ b^2)^{-1/3}}{2\pi\, f(\varepsilon)g(\varepsilon)} \left[\left(\frac{b}{\ell}\right)^2 - q^2 f^2(\varepsilon)g^2(\varepsilon)\left(1 + \frac{2}{3}\ln\left(\frac{b}{r_+}\right)\right) \right], \\ \qquad \text{for } \alpha = \pm 1, \\ \frac{2\alpha^2+1}{2\pi\, f(\varepsilon)g(\varepsilon)} \left[\frac{b}{\ell^2}\left(\frac{b}{r_+}\right)^{\frac{2\alpha^2-1}{2\alpha^2+1}} + \frac{q^2 f^2(\varepsilon)g^2(\varepsilon)}{b(\alpha^2-1)}\left(\frac{b}{r_+}\right)^{\frac{1}{2\alpha^2+1}} \right], \\ \qquad \text{for } \alpha \neq \pm 1, \end{cases}
$$
(3.14)

in which, the mass parameter m has been eliminated by use of the relation $U(r_+) = 0$.

In the case $\alpha = 0$ and $\varepsilon \to 0$ the black hole temperature coincides with that of charged BTZ black holes. It must be noted that extreme black holes occur if q and r_+ be chosen such that $T = 0$. With this issue in mind, making use of Eq. (3.14) we have

$$
r_{1\,ext} = \begin{cases} b \exp\left[\frac{3}{2}\left(1 - \left(\frac{b}{\ell q f(\varepsilon)g(\varepsilon)}\right)^2\right)\right], & \text{for } \alpha = \pm 1, \\ b\left[\frac{b^2(1-\alpha^2)}{q^2\ell^2 f^2(\varepsilon)g^2(\varepsilon)}\right]^{\frac{2\alpha^2+1}{2(\alpha^2-1)}}, & \text{for } \alpha \neq \pm 1. \end{cases}
$$
(3.15)

In order to investigate the effects of rainbow functions on the horizon temperature the plots of black hole temperature versus horizon radius have been shown in Figs. 3 and 4. The physical black

holes with positive temperature are those for which $r_+ > r_{1\,ext}$ and un-physical black holes, having negative temperature, occur if $r_+ < r_{1\,ext}$. An important point is that for the black holes correspond to $\alpha \neq \pm 1$, it is possible to fix the parameter such that $r_{1\,ext}$ does not exist. In this cases, which is not shown in the plots, the black hole temperature is positive valued and extreme or un-physical black holes do not appear.

Next, we calculate the entropy of the black holes. It can be obtained from Hawking–Bekenstein entropy-area law, that is

$$
S = \frac{A}{4} = \begin{cases} \frac{\pi r_+}{2\, g(\varepsilon)}\left(\frac{b}{r_+}\right)^{2/3}, & \text{for } \alpha = \pm 1, \\ \frac{\pi r_+}{2\, g(\varepsilon)}\left(\frac{b}{r_+}\right)^{2\alpha\gamma}, & \text{for } \alpha \neq \pm 1. \end{cases}
$$
(3.16)

Also, the black hole's electric potential on the horizon, measured by an observer at the reference point, can be obtained in terms of the null generator of the horizon $\chi^\mu = C\partial^\mu$, as

$$
\Phi = A_\mu \chi^\mu|_{\text{reference}} - A_\mu \chi^\mu|_{r=r_+}.
$$
(3.17)

Noting Eq. (3.1) we have

$$
\Phi = Cq \ln\left(\frac{r_+}{\ell}\right),
$$
(3.18)

where C is a constant coefficient [42–44].

We are now in the position to check the validity of the first law of black hole thermodynamics for both of the new rainbow black hole solutions obtained in this section. To do so, making use of Eqs. (3.7), (3.12), (3.13) and (3.16), we can obtain the black hole mass as the function of extensive parameters S and Q that is
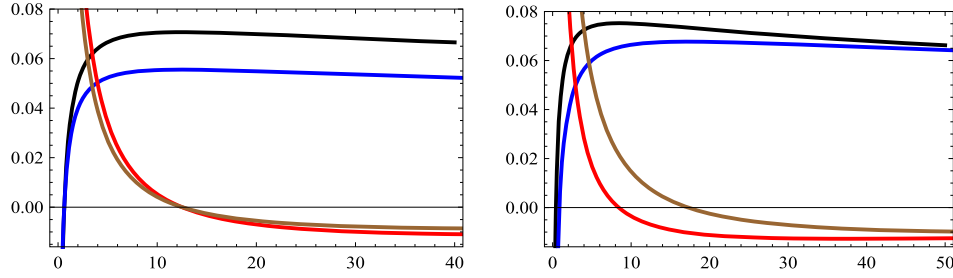
Fig. 3. $0.1T$ and $(\partial^2 M/\partial S^2)_Q$ versus r_+ for $\alpha = \pm 1$, $\ell = 1$, $Q = 1$ and $b = 2$, Eqs. (3.14) and (3.24). Left: $g(\varepsilon) = 0.75$, ($0.1T$, $f(\varepsilon) = 1.1$, 1.4 for black and blue curves, respectively) and (($\partial^2 M/\partial S^2)_Q$, $f(\varepsilon) = 1.1$, 1.4 for red and brown curves, respectively). Right: $f(\varepsilon) = 1.1$, ($0.1T$, $g(\varepsilon) = 0.7$, 0.8 for black and blue curves, respectively) and (($\partial^2 M/\partial S^2)_Q$, $g(\varepsilon) = 0.7$, 0.8 for red and brown curves, respectively). (For interpretation of the references to color in this figure legend, the reader is referred to the web version of this article.)
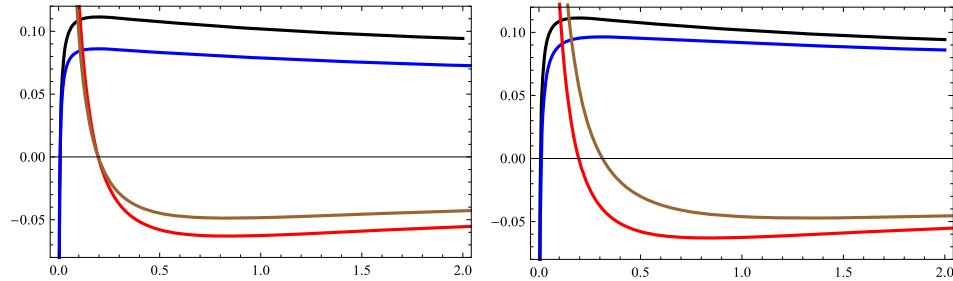
Fig. 4. $0.1T$ and $(\partial^2 M/\partial S^2)_Q$ versus r_+ for $\alpha \neq \pm 1$, $\ell = 1$, $Q = 0.5$ $\alpha = 0.9$ and $b = 2$, Eqs. (3.14) and (3.24). Left: $g(\varepsilon) = 0.58$, ($0.1T$, $f(\varepsilon) = 0.85$, 1.1 for black and blue curves, respectively) and (($\partial^2 M/\partial S^2)_Q$, $f(\varepsilon) = 0.85$, 1.1 for red and brown curves, respectively). Right: $f(\varepsilon) = 0.85$, ($0.1T$, $g(\varepsilon) = 0.58$, 0.6 for black and blue curves, respectively) and (($\partial^2 M/\partial S^2)_Q$, $g(\varepsilon) = 0.58$, 0.6 for red and brown curves, respectively). (For interpretation of the references to color in this figure legend, the reader is referred to the web version of this article.)

$$M(S, Q) = \begin{cases} \frac{1}{4f(\varepsilon)g^2(\varepsilon)}\left[\frac{b^2}{\ell^2} - 4Q^2 g^2(\varepsilon)\left(1 + \frac{1}{3}\ln\frac{b^2}{\ell r_+(S)}\right)\right] \\ \qquad \times \ln\frac{r_+(S)}{\ell}, \qquad \text{for} \quad \alpha = \pm 1, \\ \frac{2\alpha^2+1}{8f(\varepsilon)g^2(\varepsilon)(\alpha^2-1)}\left[\Lambda b_+^2(S)\left(\frac{b}{r_+(S)}\right)^{2(3\alpha\gamma-1)}\right. \\ \qquad \left. + \frac{8Q^2 g^2(\varepsilon)}{2\alpha^2+1}\ln\left(\frac{r_+(S)}{\ell}\right)\right], \quad \text{for} \quad \alpha \neq \pm 1. \end{cases} \tag{3.19}$$

Note that, if we set $\alpha = 0$ and take the infrared limit of the theory, the mass of the black hole reduces to

$$m = 8M = \frac{r_+^2}{\ell^2} - 2q^2 \ln\left(\frac{r_+}{\ell}\right), \tag{3.20}$$

which is compatible with that of charged BTZ black holes. Now, we obtain the intensive parameters T and Φ, conjugate to the black hole entropy and charge, respectively. It is a matter of calculation to show that

$$\left(\frac{\partial M}{\partial S}\right)_Q = T \qquad \text{and} \qquad \left(\frac{\partial M}{\partial Q}\right)_S = \Phi, \tag{3.21}$$

provided that C be equal to $(\alpha^2 - 1)^{-1}$ in Eq. (3.18) for the cases $\alpha \neq \pm 1$. Also, Eq. (3.21) is valid for the case $\alpha = \pm 1$ if we set $C = -1$ and the horizon radius be restricted through the relation $b^2 = \ell r_+$ [36,42–44]. Therefore, we proved that the first law of black hole thermodynamics is valid for both classes of the new EMd black holes in the following form

$$dM(S, Q) = TdS + \Phi dQ. \tag{3.22}$$

3.2. Heat capacity and stability analysis

In this stage, we would like to study the local stability or phase transition of the new black hole solutions in the canonical ensemble method. It is well-known that a black hole, as a thermodynam-

ical system, is locally stable if its heat capacity is positive. A non-stable black hole undergoes phase transition to be stabilized. The points of phase transition are where the black hole heat capacity vanishes or diverges. The vanishing points or the real roots of the black hole heat capacity are known as the points of type one phase transition. The divergent points or the real roots of the denominator of the black hole heat capacity are the points at which type two phase transitions take place. The black hole heat capacity, calculated in the fixed black hole's charge, is defined as

$$C_Q = T\frac{\partial S}{\partial T} = T\left(\frac{\partial^2 M}{\partial S^2}\right)^{-1}. \tag{3.23}$$

The last step in Eq. (3.23) comes from the fact that $T = \partial M/\partial S$. Therefore, the positivity of heat capacity $C_Q = T(\partial S/\partial T)_Q = T/(\partial^2 M/\partial S^2)_Q$ or equivalently the positivity of $(\partial S/\partial T)_Q$ or $(\partial^2 M/\partial S^2)_Q$ with $T > 0$ are sufficient to ensure the local stability of the black hole [34–38].

In order to perform a black hole stability analysis we need to have the explicit form of the black hole heat capacity. The numerator of the black hole heat capacity is given in Eq. (3.14). Now, we calculate the denominator of the black hole heat capacity. It can be written as

$$\left(\frac{\partial^2 M}{\partial S^2}\right)_Q = \begin{cases} \frac{2q^2 f(\varepsilon)g^2(\varepsilon)}{\pi^2 b^2}\left(\frac{b}{r_+}\right)^{2/3}\left[\frac{2}{3}\ln\frac{b}{r_+} + 3\right. \\ \qquad \left. - \left(\frac{b}{q\ell f(\varepsilon)g(\varepsilon)}\right)^2\right], \qquad \text{for} \quad \alpha = \pm 1, \\ \frac{1+2\alpha^2}{\pi^2\ell^2 f(\varepsilon)}\left[(1 - 2\alpha^2)\left(\frac{b}{r_+}\right)^{\frac{2\alpha^2}{1+2\alpha^2}}\right. \\ \qquad \left. - \frac{q^2 f^2(\varepsilon)g^2(\varepsilon)\ell^2}{b^2(\alpha^2-1)}\left(\frac{b}{r_+}\right)^{\frac{2}{1+2\alpha^2}}\right], \\ \qquad \text{for} \quad \alpha \neq \pm 1. \end{cases} \tag{3.24}$$

It is understood from Eq. (3.23) that if

$$r_+ \equiv r_0 = \begin{cases} b \exp\left[\frac{3}{2}\left(3 - \left(\frac{b}{q\ell f(\varepsilon)g(\varepsilon)}\right)^2\right)\right], & \text{for} \quad \alpha = \pm 1, \\ b\left[\frac{b^2(1-\alpha^2)(2\alpha^2-1)}{q^2\ell^2 f^2(\varepsilon)g^2(\varepsilon)}\right]^{\frac{1+2\alpha^2}{2(\alpha^2-1)}}, & \text{for} \quad \alpha \neq \pm 1. \end{cases}$$
(3.25)

According to Eqs. (3.15) and (3.25), r_{1ext} and r_0 are always exist for the case $\alpha = \pm 1$ and $r_0 > r_{1ext}$. Therefore, the points of type one and type two phase transitions are located at $r_+ = r_{1ext}$ and $r_+ = r_0$, respectively. Also, this class of new black holes are locally stable if their horizon radius is in the range $r_{1ext} < r_+ < r_0$. The plots Fig. 3 show the impacts of rainbow functions on the numerator and denominator of the black hole heat capacity.

For the black holes with $\alpha \neq \pm 1$ it is possible to fix the parameters such that both r_{ext} and r_0 exist, simultaneously. If it is the case, type one and type two phase transitions take place at $r_+ = r_{ext}$ and $r_+ = r_0$, respectively. This class of black holes with the horizon radius in the range $r_{1ext} < r_+ < r_0$ are locally stable (Fig. 4). In addition, there are two following possibilities which are not shown in the figures. One is correspond to the case r_0 exists but r_{1ext} does not. In this case, the black hole temperature is positive valued and no type one phase transition can occur. There is type two phase transition located at $r_+ = r_0$ and black holes with the horizon radius greater than r_0 are locally stable. The other corresponds to the case r_{1ext} exists but r_0 does not. The denominator of the black hole heat capacity is positive valued and no type two phase transition takes place. The black holes with $r_+ = r_{1ext}$ undergo type one phase transition to be stabilized. Also, the black holes with the horizon radius in the range $r_+ > r_{1ext}$ are locally stable.

4. Black hole solutions with $\beta \neq \alpha$

In order to obtain the black hole solutions correspond to the case $\beta \neq \alpha$, we start with the electromagnetic field equation (2.3). Regarding Eqs. (2.5) and (2.13), it can be solved, we have

$$\begin{cases} h(r) = -\frac{q}{A} r^{-A}, & \text{and} \quad A = 2\gamma(\alpha - \beta), \\ F_{tr} = q\, r^{-(1+A)}, \end{cases}$$
(4.1)

where, q is an integration constant related to the total electric charge on black hole. In order to the potential function $A_\mu = h(r)\delta_\mu^0$ be physically reasonable (i.e. zero at infinity), the statement $A = 2\gamma(\alpha - \beta)$ must be positive. Thus we suppose that $\alpha > \beta$ with both α and β positive. The electric field (4.1) can be regarded as a modified Coulomb's electric field.

Now, Eq. (2.9) can be rewritten as

$$U'(r) - \frac{2\beta\gamma}{r} U(r) + \frac{r}{(1-2\beta\gamma)g^2(\varepsilon)}$$
$$\times \left[V(\phi) + 2f^2(\varepsilon)g^2(\varepsilon)F_{tr}^2 e^{-2\alpha\phi}\right] = 0,$$
(4.2)

and the scalar field equation (2.4) takes the following form

$$\frac{dV(\phi)}{d\phi} - 4\beta V(\phi) - 4(2\beta - \alpha)f^2(\varepsilon)g^2(\varepsilon)F_{tr}^2 e^{-2\alpha\phi} = 0.$$
(4.3)

Noting Eq. (4.1), the first order differential (4.3) can be solved as

$$V(\phi) = 2\Lambda e^{4\beta\phi} + 2\Lambda_0 e^{4\beta_0\phi},$$
(4.4)

where

$$\Lambda_0 = \frac{q^2(\Upsilon - 1)}{b^{2(A+1)}} f^2(\varepsilon)g^2(\varepsilon) \quad \text{and} \quad \Upsilon = (1 + \alpha\beta - 2\beta^2)^{-1}$$
$$\text{and} \quad \beta_0 = \frac{1 + \alpha\beta}{2\beta}.$$
(4.5)

It is notable that the solution given by Eq. (4.4) can be considered as the generalized form of the Liouville scalar potential. Also, it must be noted that in the absence of dilatonic field ϕ, we have $V(\phi = 0) = 2\Lambda = -2\ell^{-2}$ and the action (2.1) reduces to that of Einstein-Λ-Maxwell theory.

By substituting $F_{tr}(r)$ and $V(r)$ from Eqs. (4.1) and (4.4) into Eq. (4.2), we arrived at the metric function $U(r)$ as

$$U(r) = \begin{cases} -m\, r^{2/3} - \frac{6b^2}{g^2(\varepsilon)}\left(\frac{r}{b}\right)^{2/3}\left[\Lambda \ln\left(\frac{r}{\ell}\right)\right. \\ \left. - \frac{3q^2 f^2(\varepsilon)g^2(\varepsilon)}{2b^2(\alpha-1)^2}(br)^{\frac{2}{3}(1-\alpha)}\right], \\ \quad \text{for} \quad \beta = 1, \quad \alpha > 1 \\ -m\, r^{2\beta\gamma} - \frac{(1+2\beta^2)^2}{g^2(\varepsilon)}\left[\frac{\Lambda r^2}{1-\beta^2}\left(\frac{b}{r}\right)^{4\beta\gamma}\right. \\ \left. + \frac{q^2 f^2(\varepsilon)g^2(\varepsilon)\Upsilon b^{-2A}}{\beta(\beta-\alpha)}\left(\frac{b}{r}\right)^{2\gamma(\alpha-2\beta)}\right], \\ \quad \text{for} \quad \beta \neq 1, \quad \alpha > \beta. \end{cases}$$
(4.6)

The plots of metric functions $U(r)$, presented in Eq. (4.6), for $\beta = 1$ and $\beta \neq 1$ cases have been shown in Figs. 5 and 6, respectively. They show the effects of rainbow functions on the metric function $U(r)$ for the cases $\beta = 1$ and $\beta \neq 1$. From the curves of Figs. 5 and 6, it is obvious that the metric function $U(r)$ can produce two horizon, extreme and naked singularity black holes for both of $\beta = 1$ and $\beta \neq 1$ cases.

Investigation of the curvature singularities through the Ricci and Kretschmann scalars show that their asymptotic behaviors fulfill the Eqs. (3.9) and (3.10). It means that there is an essential singularity located at $r = 0$ and the asymptotic behavior of the black holes correspond to the case $\beta \neq \alpha$ are also non-flat non-AdS.

4.1. First law of black hole thermodynamics

Here, we tend to check the validity of the first law of black hole thermodynamics for the new dilatonic black holes correspond to the case $\beta \neq \alpha$. Making use of Eq. (3.11), the conserved charge of the black hole can be obtained as

$$Q = \frac{qf(\varepsilon)}{2} b^{-A}.$$
(4.7)

The black hole mass as the other conserved quantity to be calculated in terms of the mass parameter m. It is a matter of calculation to show that the Abbott–Deser total mass of the new rainbow charged dilatonic BTZ black holes introduced here can be obtained as

$$M = \begin{cases} \frac{mb^{2/3}}{24f(\varepsilon)}, & \text{for} \quad \beta = 1, \\ \frac{mb^{2\beta\gamma}}{8f(\varepsilon)(1+2\beta^2)}, & \text{for} \quad \beta \neq 1, \end{cases}$$
(4.8)

which is compatible with the mass of charged BTZ black hole in the absence of rainbow functions [35].

Also, the Hawking temperature associated with the black hole horizon $r = r_+$, can be calculated in terms of the surface gravity κ. It is easy to show that
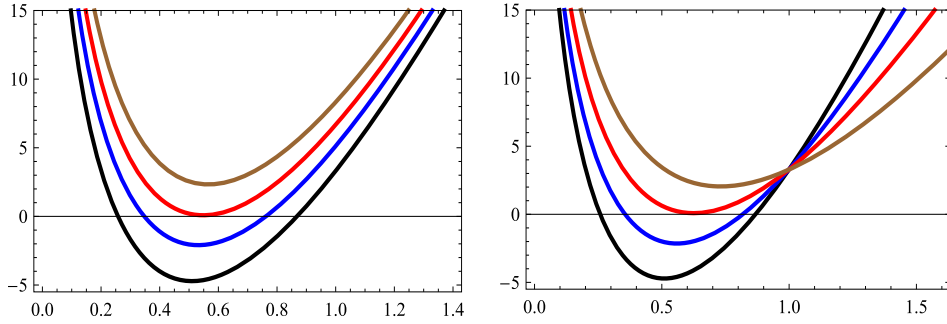
Fig. 5. $U(r)$ versus r for $\beta = 1$, $\Lambda = -1$, $Q = 1$, $M = 2.5$, $\alpha = 2.2$ and $b = 3$, Eq. (4.6). Left: $g(\varepsilon) = 0.7$ and $f(\varepsilon) = 1.1$, 1.15, 1.19, 1.23, Right: $f(\varepsilon) = 1.1$ and $g(\varepsilon) = 0.7$, 0.745, 0.798, 0.87, for Black, blue, red, and brown curves, respectively. (For interpretation of the references to color in this figure legend, the reader is referred to the web version of this article.)

Fig. 6. $U(r)$ versus r for $\beta = 0.5$, $\Lambda = -1$, $Q = 1$, $M = 2$, $\alpha = 2$ and $b = 2$, Eq. (4.6). Left: $g(\varepsilon) = 0.8$ and $f(\varepsilon) = 0.5$, 0.635, 0.78, 0.9, Right: $f(\varepsilon) = 1$ and $g(\varepsilon) = 0.45$, 0.512, 0.58, 0.65, for Black, blue, red, and brown curves, respectively. (For interpretation of the references to color in this figure legend, the reader is referred to the web version of this article.)
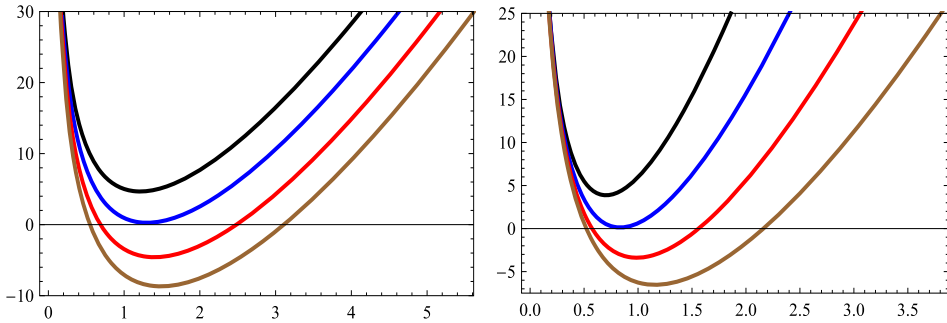
$$
T = \frac{\kappa}{2\pi} = \frac{g(\varepsilon)}{f(\varepsilon)} \frac{U'(r_+)}{4\pi}
$$

$$
= \begin{cases}
-\dfrac{3b\Lambda}{2\pi f(\varepsilon)g(\varepsilon)} \left(\dfrac{b}{r_+}\right)^{1/3} \left[1 + \dfrac{q^2 f^2(\varepsilon)g^2(\varepsilon)b^{(1-4\alpha)/3}}{b\Lambda(\alpha-1)} \left(\dfrac{b}{r_+}\right)^{\frac{2}{3}(\alpha-1)}\right], \\
\qquad \text{for} \quad \beta = 1, \\[2mm]
-\dfrac{(1+2\beta^2)\Lambda r_+}{2\pi f(\varepsilon)g(\varepsilon)} \left[\left(\dfrac{b}{r_+}\right)^{4\beta\gamma} + \dfrac{q^2 f^2(\varepsilon)g^2(\varepsilon)\Upsilon}{\Lambda r_+^2 b^{2A}} \left(\dfrac{b}{r_+}\right)^{2\gamma(\alpha-2\beta)}\right], \\
\qquad \text{for} \quad \beta \neq 1.
\end{cases}
$$

(4.9)

Extreme black holes may occur if the real roots of $T = 0$ exist. The horizon radius of the extreme black holes can be obtained as

$$
r_{2\,ext} = \begin{cases}
\left(\dfrac{q^2 f^2(\varepsilon)g^2(\varepsilon)\ell^2}{\alpha-1}\right)^{\frac{3}{2(\alpha-1)}} b^{\frac{\alpha+2}{1-\alpha}}, & \text{for} \quad \beta = 1,\ \alpha > 1, \\[3mm]
b \left(\dfrac{q^2 f^2(\varepsilon)g^2(\varepsilon)\ell^2 \Upsilon}{b^{2(1+A)}}\right)^{\frac{\Upsilon}{2}(1+2\beta^2)}, & \text{for} \quad \beta \neq 1.
\end{cases}
$$

(4.10)

In order to the effects of rainbow functions on the horizon temperature of the black holes be studied more closely, we have plotted them in Figs. 7 and 8 for $\beta = 1$ and $\beta \neq 1$ cases, respectively. The plots show that, for the proper choice of the parameters, physical and un-physical black holes occur for $r_+ > r_{2\,ext}$ and $r_+ < r_{2\,ext}$, respectively. A notable point is that in the case $\beta = 1$, $r_+ = r_{2\,ext}$ exists always, while in the case $\beta \neq 1$ it is possible to fix the parameters such that $r_+ = r_{2\,ext}$ does not exist. If it is the case, the black hole temperature is positive valued and no extreme or un-physical black hole can occur.

The Hawking–Bekenstein entropy of the black holes takes the following form

$$
S = \frac{A}{4} = \begin{cases}
\dfrac{\pi b}{2g(\varepsilon)} \left(\dfrac{r_+}{b}\right)^{1/3}, & \text{for} \quad \beta = 1, \\[3mm]
\dfrac{\pi b}{2g(\varepsilon)} \left(\dfrac{r_+}{b}\right)^{1-2\beta\gamma}, & \text{for} \quad \beta \neq 1.
\end{cases}
$$

(4.11)

Noting Eqs. (3.17) and (4.1), one can show that the black hole's electric potential Φ can be written as

$$
\Phi = \begin{cases}
\dfrac{3Cq}{2(\alpha-1)} r_+^{-\frac{2}{3}(\alpha-1)}, & \text{for} \quad \beta = 1, \\[3mm]
\dfrac{Cq}{A} r_+^{-A}, & \text{for} \quad \beta \neq 1.
\end{cases}
$$

(4.12)

In order to investigate the consistency of these quantities with the thermodynamical first law, we can write the relation corresponding Smarr-type mass formula as

$$
M(S, Q) = \begin{cases}
\dfrac{1}{4f(\varepsilon)g^2(\varepsilon)} \left[\dfrac{b^2}{\ell^2} \ln\left(\dfrac{\ell}{r_+(S)}\right)\right. \\
\qquad \left. + \dfrac{6Q^2 g^2(\varepsilon)}{(\alpha-1)^2} \left(\dfrac{b}{r_+(S)}\right)^{\frac{2}{3}(\alpha-1)}\right], \\
\qquad \text{for} \quad \beta = 1, \\[3mm]
-\dfrac{1+2\beta^2}{8f(\varepsilon)g^2(\varepsilon)} \left[\dfrac{\Lambda b^2}{1-\beta^2} \left(\dfrac{b}{r_+(S)}\right)^{2(3\beta\gamma-1)}\right. \\
\qquad \left. + \dfrac{4\Upsilon Q^2 g^2(\varepsilon)}{\beta(\beta-\alpha)} \left(\dfrac{b}{r_+(S)}\right)^A\right], & \text{for} \quad \beta \neq 1,
\end{cases}
$$

(4.13)

from which one can calculate the intensive parameters T and Φ, conjugate to the black hole entropy and charge, respectively. It can be shown that

$$
\left(\frac{\partial M}{\partial S}\right)_Q = T, \quad \text{and} \quad \left(\frac{\partial M}{\partial Q}\right)_S = \Phi,
$$

(4.14)

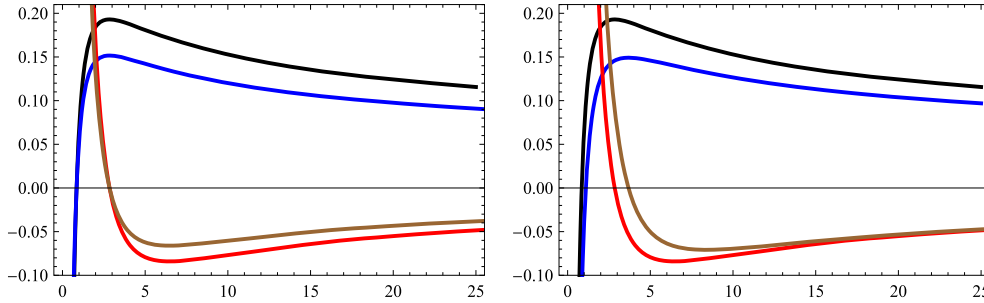provided that C be chosen as $C = \Upsilon$ [42–44].

Fig. 7. $0.25T$ and $(\partial^2 M/\partial S^2)_Q$ versus r_+ for $\beta = 1$, $\ell = 1$, $Q = 1$, $\alpha = 3$ and $b = 2$, Eqs. (4.9) and (4.15). Left: $g(\varepsilon) = 0.8$, $(0.25T$, $f(\varepsilon) = 1.1$, 1.4 for black and blue curves, respectively) and $((\partial^2 M/\partial S^2)_Q$, $f(\varepsilon) = 1.1$, 1.4 for red and brown curves, respectively). Right: $f(\varepsilon) = 1.1$, $(0.25T$, $g(\varepsilon) = 0.8$, 0.95 for black and blue curves, respectively) and $((\partial^2 M/\partial S^2)_Q$, $g(\varepsilon) = 0.8$, 0.95 for red and brown curves, respectively). (For interpretation of the references to color in this figure legend, the reader is referred to the web version of this article.)
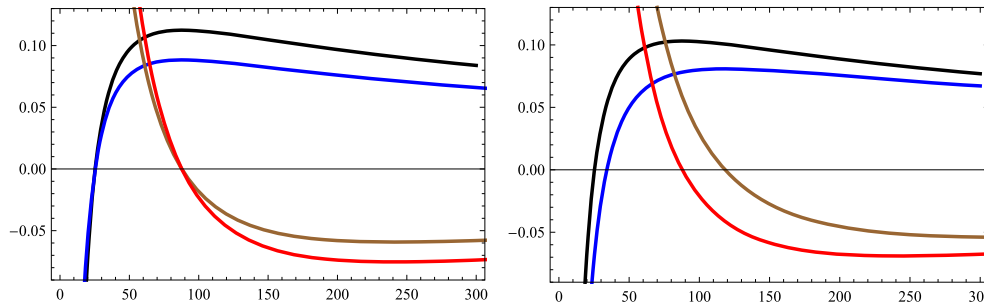

Fig. 8. T and $5(\partial^2 M/\partial S^2)_Q$ versus r_+ for $\beta \neq 1$, $\ell = 1$, $Q = 1$, $\alpha = 3$, $\beta = 1.5$ and $b = 3$, Eqs. (4.9) and (4.15). Left: $g(\varepsilon) = 0.9$, $(T$, $f(\varepsilon) = 1.1$, 1.4 for black and blue curves, respectively) and $(5(\partial^2 M/\partial S^2)_Q$, $f(\varepsilon) = 1.1$, 1.4 for red and brown curves, respectively). Right: $f(\varepsilon) = 1.2$, $(T$, $g(\varepsilon) = 0.9$, 0.95 for black and blue curves, respectively) and $(5(\partial^2 M/\partial S^2)_Q$, $g(\varepsilon) = 0.9$, 0.95 for red and brown curves, respectively). (For interpretation of the references to color in this figure legend, the reader is referred to the web version of this article.)

It shows that the first law of black hole thermodynamics, in the following form of Eq. (3.22), is valid for both classes of the new charged dilatonic BTZ black holes in rainbow gravity.

4.2. Heat capacity and stability analysis

Here, regarding the issues mentioned in subsection 3.2, we perform a black hole stability or phase transition analysis for both of the new rainbow charged dilatonic BTZ black holes, we just obtained. Using Eq. (4.13), we have obtained the denominator of the black hole heat capacity as

$$
\left(\frac{\partial^2 M}{\partial S^2} \right)_Q =
\begin{cases}
\frac{3}{\pi^2 f(\varepsilon)} \left(\frac{b}{r_+} \right)^{2/3} \left[\Lambda + q^2 f^2(\varepsilon) g^2(\varepsilon) \left(\frac{2\alpha - 1}{\alpha - 1} \right) \right. \\
\left. \times b^{-\frac{2}{3}(2\alpha+1)} \left(\frac{b}{r_+} \right)^{\frac{2}{3}(\alpha-1)} \right], \\
\quad \text{for} \quad \beta = 1, \\
\frac{1+2\beta^2}{\pi^2 f(\varepsilon)} \left[\Lambda (2\beta^2 - 1) \left(\frac{b}{r_+} \right)^{2\beta\gamma} \right. \\
\left. + \frac{q^2 f^2(\varepsilon) g^2(\varepsilon)(1+\alpha\beta\Upsilon)}{b^{2(1+A)}} \left(\frac{b}{r_+} \right)^{\frac{2\gamma}{\beta}(1+\alpha\beta-\beta^2)} \right], \\
\quad \text{for} \quad \beta \neq 1.
\end{cases}
\tag{4.15}
$$

In order to study of the divergent points of the black hole heat capacity, as the points of the type two phase transition, we need to have the real roots of $(\partial^2 M/\partial S^2)_Q = 0$. As a matter of calculation, they can be obtained in the following form

$$
r_+ \equiv r_1 =
\begin{cases}
\left[q^2 f^2(\varepsilon) g^2(\varepsilon) \ell^2 \left(\frac{2\alpha-1}{\alpha-1} \right) \right]^{\frac{3}{2(\alpha-1)}} b^{\frac{\alpha+2}{1-\alpha}}, \\
\quad \text{for} \quad \beta = 1, \quad \alpha > 1, \\
b \left[\frac{q^2 f^2(\varepsilon) g^2(\varepsilon) \ell^2 (1+\alpha\beta\Upsilon)}{(2\beta^2-1) b^{2(1+A)}} \right]^{\frac{\Upsilon}{2}(1+2\beta^2)} \\
\quad \text{for} \quad \beta \neq 1.
\end{cases}
\tag{4.16}
$$

Now, it must be noted that $r_{2\,ext}$ and r_1 always exist and $r_1 > r_{2\,ext}$ for the case $\beta = 1$. Therefore, this class of new rainbow black holes undergo type one and type two phase transitions at $r_+ = r_{2\,ext}$ and $r_+ = r_1$, respectively. They are locally stable if their horizon radiuses are in the range $r_{2\,ext} < r_+ < r_1$. The plots of numerator and denominator of the heat capacity versus r_+ are shown in Fig. 7, for different values of rainbow functions and $\beta = 1$.

Also, Fig. 8 shows the plots of numerator and denominator of the black hole heat capacity versus r_+ for different values of rainbow functions and $\beta \neq 1$. It shows that it is possible to fix the parameters such that both $r_{2\,ext}$ and r_1 exist. In this case $r_{2\,ext}$ and r_1 are the points of type one and type two phase transitions, respectively. The black holes with the horizon radiuses in the range $r_{2\,ext} < r_+ < r_1$ are locally stable. Furthermore, for especial choice of the parameters, two following nontrivial cases can achieved which are not shown in the figures.

Case I: r_1 exists but $r_{2\,ext}$ does not. In this case, as mentioned in the previous subsection, T is positive valued and extreme or un-physical black holes do not occur. The black hole heat capacity does not vanish and no type one phase transition takes place. Also, the black hole heat capacity diverges at $r_+ = r_1$ which is the location of type two phase transition and black holes with $r_+ > r_1$ are locally stable.

Case II: $r_{2\,ext}$ exists but r_1 does not. In this case the denominator of the black hole heat capacity is positive everywhere and no type two phase transition occurs. The point $r_+ = r_{2\,ext}$, at

which the black hole heat capacity vanishes, is a point of type one phase transition. The black hole heat capacity is positive valued for $r_+ > r_{2\,ext}$ and black holes with the horizon radiuses in this range are locally stable.

5. Conclusion

In this paper, we investigated the charged dilatonic BTZ black hole solutions in the rainbow gravity theory. Starting from the suitable three-dimensional action, we obtained the explicit form of the field equations in an energy dependent static spherically symmetric geometry. We found that two kinds of electric fields can be achieved if the parameters of the theory are considered properly (i.e. $\beta \neq \alpha$ and $\beta = \alpha$). One is the well known Coulomb's electric field and the other one can be interpreted as the modification to the usual electric field which reduces to the Coulomb's field as an especial case. We proceed to obtain the black hole solutions with $\beta = \alpha$ and $\beta \neq \alpha$ cases, separately. We found that there are two new classes of rainbow black hole solutions correspond to the case $\beta = \alpha$ (Eq. (3.7)) and two other new classes of black hole solutions in the presence of modified Coulomb field (Eq. (4.7)). All the new black hole solutions can produce two horizon extreme and naked singularity black holes (Figs. 1, 2 and 5, 6). Also, there is an essential singularity located at $r = 0$ and the asymptotic behavior of the black holes are non flat and non AdS.

Next, by utilizing the Gauss's law of electricity and Abbott–Deser mass proposal, we obtained the black hole mass and electric charge for either of the four new classes of the rainbow black hole solutions. Also, we have calculated the entropy and temperature of the new black hole solutions based on the entropy-area law and concept of the surface gravity. For both classes of rainbow black holes correspond to $\beta = \alpha$ extreme black holes occur at $r_+ = r_{1\,ext}$. The physical and un-physical black holes occur for $r_+ > r_{1\,ext}$ and $r_+ < r_{1\,ext}$, respectively. In the case $\beta = \alpha \neq \pm 1$ there is an especial case for which the temperature is positive valued and extreme ore un-physical black holes do not occur. For the black hole solutions with $\beta = \alpha$ it is possible for the temperature to vanish at $r_+ = r_{2\,ext}$ and produce the extreme black holes. If it is the case, physical and un-physical black holes can occur for $r_+ > r_{2\,ext}$ and $r_+ < r_{2\,ext}$, respectively. An especial case to be mentioned is related to the case $\beta \neq \pm 1$ for which $r_{2\,ext}$ does not exist, the black hole temperature is positive valued and extreme or un-physical black holes can not occur. Through a smarr-type mass formula, which states the black hole mass as the function of the extensive parameters Q and S, we proved that thermodynamical fist law is valid for either of the new black hole solutions in the form of Eq. (3.22).

In addition, making use of the canonical ensemble method, we performed a thermal stability analysis for the new rainbow black hole solutions by considering the $\beta = \alpha$ and $\beta \neq \alpha$ cases, separately. For the black holes with $\beta = \alpha = \pm 1$, $r_{1\,ext}$ and r_0 are exist always and $r_0 > r_{1\,ext}$. As the result there is a type one phase transition located at $r_+ = r_{1\,ext}$ where the black hole heat capacity vanishes. The point $r_+ = r_0$ is the point at which the black hole heat capacity diverges and they undergo type two phase transition to be stabilized. This class of rainbow black hole solutions are locally stable if their horizon radius is in the range $r_{1\,ext} < r_+ < r_0$ (Fig. 3). For the new rainbow black hole solutions correspond to $\beta = \alpha \neq \pm 1$ three following possibilities are of interest:

(*i*) Both $r_{1\,ext}$ and r_0 are exist. In this case $r_+ = r_{1\,ext}$ and $r_+ = r_0$ are the points of type one and type two phase transitions, respectively. This class of new rainbow black holes are stable if their horizon radiuses are in the range $r_{1\,ext} < r_+ < r_0$ (Fig. 4).

(*ii*) $r_{1\,ext}$ exists but r_0 does not exist. In this case the denominator of the black hole heat capacity is positive valued and there is no type two phase transition. They undergo type one phase tran-

sition at the point $r_+ = r_{1\,ext}$ where the black hole heat capacity vanishes. The new charged rainbow black holes are locally stable if their horizon radiuses are in the range $r_+ > r_{1\,ext}$. This case is not shown in the figures.

(*iii*) r_0 exists but $r_{1\,ext}$ does not exist. The black hole temperature is positive valued. Thus, the black hole heat capacity does not vanishes and no type one phase transition takes place. There is a type two phase transition located at $r_+ = r_0$ where the black hole heat capacity diverges. The black holes with the horizon radiuses greater than r_0 are locally stable. This case also is not shown in the figures.

The other two new classes of rainbow black holes which are correspond to the case $\beta \neq \alpha$ undergo type one phase transition at the point $r_+ = r_{2\,ext}$ and the point of type two phase transition is located at $r_+ = r_1$. The black holes are in a thermally stable phase if their horizon radius is in the range $r_{2\,ext} < r_+ < r_1$ (Figs. 7 and 8). In addition, it must be noted that for these classes of black hole solutions with $\beta \neq 1$ two following possibilities are considerable which are not shown in the figures. (*I*) For a suitably fixed parameters it is possible to $r_{2\,ext}$ exists but r_1 does not. If it is the case, the denominator of the black hole heat capacity is positive everywhere and no type two phase transition takes place. The black hole heat capacity vanishes at $r_+ = r_{2\,ext}$ and it is the point of type one phase transition. This class of new rainbow black holes are stable for $r_+ > r_{2\,ext}$. (*II*) The other case, which can achieved as an especial case, is that $r_{2\,ext}$ does not exist and black hole temperature is positive everywhere. The point $r_+ = r_1$, as the real root of the denominator of the black hole heat capacity, exists and it is a point of type two phase transition. The physical black holes with the horizon radius greater than $r_+ = r_1$ are locally stable.

References

[1] D. Amati, M. Ciafaloni, G. Veneziano, Phys. Lett. B 197 (1987) 81;
V.A. Kostelecky, S. Samuel, Phys. Rev. D 39 (1989) 683.
[2] R. Gambini, J. Pullin, Phys. Rev. D 59 (1999) 124021.
[3] S.M. Carroll, J.A. Harvey, V.A. Kosteleck'y, C.D. Lane, T. Okamoto, Phys. Rev. Lett. 87 (2001) 141601.
[4] L.J. Garay, Int. J. Mod. Phys. A 10 (1995) 145;
X. Calmet, M. Graesser, S.D.H. Hsu, Phys. Rev. Lett. 93 (2004) 211101.
[5] D.J. Gross, P.F. Mende, Nucl. Phys. B 303 (1988) 407;
M. Maggiore, Phys. Lett. B 304 (1993) 65.
[6] P. Horava, Phys. Rev. D 79 (2009) 084008;
P. Horava, Phys. Rev. Lett. 102 (2009) 161301.
[7] S.h. Hendi, Gen. Relativ. Gravit. 48 (2016) 50.
[8] G. Amelino-Camelia, Phys. Lett. B 510 (2001) 255;
G. Amelino-Camelia, Int. J. Mod. Phys. D 11 (2002) 35.
[9] J. Magueijo, L. Smolin, Phys. Rev. Lett. 88 (2002) 190403.
[10] V.A. Kostelecky, S. Samuel, Phys. Rev. D 39 (1989) 683.
[11] J. Magueijo, L. Smolin, Class. Quantum Gravity 21 (2004) 1725;
J. Magueijo, L. Smolin, Phys. Rev. D 71 (2005) 026010.
[12] Z-W. Feng, S-Z. Yang, Phys. Lett. B 772 (2017) 737.
[13] J. Magueijo, L. Smolin, Phys. Rev. D 67 (2003) 044017.
[14] G. Amelino-Camelia, Living Rev. Relativ. 16 (2013) 5;
G. Amelino-Camelia, J.r. Ellis, N. Mavromatos, D.V. Nanopoulos, Int. J. Mod. Phys. A 12 (1997) 607.
[15] G. Amelino-Camelia, J.R. Ellis, N.E. Mavromatos, D.V. Nanopoulos, S. Sarkar, Nature 393 (1998) 763.
[16] Y. Ling, X. Li, H. Zhang, Mod. Phys. Lett. A 36 (2007) 2749.
[17] S.H. Hendi, S. Panahiyan, B. Eslam Panah, M. Momennia, Eur. Phys. J. C 76 (2016) 150;
S.H. Hendi, S. Panahiyan, B. Eslam Panah, M. Momennia, Eur. Phys. J. C 77 (2017) 647.
[18] S. Alsaleh, Int. J. Mod. Phys. A 32 (2017) 1750076.
[19] S.H. Hendi, M. Faizal, Phys. Rev. D 92 (2015) 044027.

[20] S.H. Hendi, S. Panahiyan, B. Eslam Panah, M. Faizal, M. Momennia, Phys. Rev. D 94 (2016) 044028.
[21] S.H. Hendi, S. Panahiyan, S. Upadhyay, B. Eslam, Phys. Rev. D 95 (2017) 084036;
S.H. Hendi, B. Eslam Panah, S. Panahiyan, J. High Energy Phys. 05 (2016) 029;
S.H. Hendi, B. Eslam Panah, S. Panahiyan, Phys. Lett. B 769 (2017) 191.
[22] A.F. Ali, M. Faizal, M.M. Khalile, Nucl. Phys. B 894 (2015) 341.
[23] A.F. Ali, Phys. Rev. D 89 (2014) 104040.
[24] S.H. Hendi, M. Momennia, B. Eslam Panah, M. Faizal, Astrophys. J. 827 (2016) 153.
[25] B. Pourhassan, M. Faizal, S. Upadhyay, L. Al Asfar, Eur. Phys. J. C 77 (2017) 555.
[26] S. Upadhyay, B. Pourhassan, H. Farahani, Phys. Rev. D 95 (2017) 106014.
[27] B. Pourhassan, S. Upadhyay, H. Saadat, H. Farahani, arXiv:1705.03005.
[28] B. Pourhassan, S. Upadhyay, H. Farahani, arXiv:1701.08650.
[29] S. Upadhyay, B. Pourhassan, arXiv:1711.04254.
[30] S. Upadhyay, Phys. Lett. B 775 (2017) 130.
[31] M. Dehghani, Phys. Lett. B 749 (2015) 125.
[32] S.H. Hendi, B. Eslam Panah, S. Panahiyan, Prog. Theor. Exp. Phys. 2016 (10) (2016) 103A02.
[33] S.H. Hendi, Mir Faizal, B. Eslam Panah, S. Panahiyan, Eur. Phys. J. C 76 (2016) 296.
[34] S.H. Hendi, B. Eslam Panah, S. Panahiyan, A. Sheykhi, Phys. Lett. B 767 (2017) 214.
[35] M. Dehghani, Phys. Lett. B 773 (2017) 105.
[36] M. Dehghani, Phys. Rev. D 96 (2017) 044014.
[37] A. Sheykhi, Phys. Rev. D 86 (2012) 024013.
[38] M. Dehghani, Phys. Rev. D 94 (2016) 104071;
M. Dehghani, S.F. Hamidi, Phys. Rev. D 96 (2017) 044025.
[39] L.F. Abbott, S. Deser, Nucl. Phys. B 195 (1982) 76.
[40] R. Olea, J. High Energy Phys. 06 (2005) 023.
[41] G. Kofinas, R. Olea, Phys. Rev. D 74 (2006) 084035.
[42] M. Kord Zangeneh, A. Sheykhi, M.H. Dehghani, Phys. Rev. D 91 (2015) 044035.
[43] M. Kord Zangeneh, A. Sheykhi, M.H. Dehghani, Phys. Rev. D 92 (2015) 024050.
[44] M. Kord Zangeneh, A. Sheykhi, M.H. Dehghani, Eur. Phys. J. C 75 (2015) 497.